INTERNATIONAL CONFERENCE
ON NUCLEAR POWER AND ITS FUEL CYCLE
SALZBURG, AUSTRIA • 2–13 MAY 1977

IAEA-CN-36/108

ADVANCES IN CARBIDE FUEL ELEMENT DEVELOPMENT FOR FAST REACTOR APPLICATION

W.Dienst, H.Kleykamp, G.Mühling, H.Reiser,
H.Steiner, F.Thümmler, H.Wedemeyer, P.Weimar

Kernforschungszentrum Karlsruhe
Institut für Material- und Festkörperforschung
Projekt Schneller Brüter
Federal Republic of Germany

PROGRAM REVIEW AND FUEL PIN CONCEPT

Since 1968 a research program has been performed at GfK to develop a carbide fuel element for use in the German SNR-300 Breeder Reactor. The main objectives of this program are:

- Development of a suitable fuel fabrication process for mixed (U,Pu)-carbide in cooperation with the German industrial fuel fabricators.
- Basic research to obtain specific material data as for irradiation creep and swelling of (U,Pu)-carbide.
- Planning, design, construction and performance of irradiation experiments. Within this part of the program, about 50 single-pin irradiations were already performed; irradiation of original-sized fuel elements in KNK-II and non-steady-state tests are foreseen for the near future. A survey on status and planning is given in Fig. 1.
- Post-irradiation examinations and evaluation of data, complemented by theoretical work in the field of fuel pin modelling and its application.

Based on our own and international irradiation results a reference carbide-pin design has been chosen. The main data are given in Table I.

The selection of this reference concept was made for the following reasons:

- The pin design with pelletized fuel and He-bonding is more simple and cheaper, with respect to fabrication, than a concept with Na-bonding. The fabrication steps are very similar to oxide pin preparation and are based on reliable procedures and technological experience.
- Taking into account the very moderate concept conditions (fuel density, linear rod-power and burn-up), no unsolvable problems with regard to fuel- or clad-swelling are expected.
- In spite of those moderate conditions, breeding ratio (which is still remarkably better than with oxide), fissile inventory and doubling-time are still satisfactory.

In addition to the reference concept two alternatives are examined with a small effort. These are the pin concept with vibrocompacted fuel and He-bonding which offers promise of easier fabrication, and the concept with pelletized fuel and Na-bonding for extended use of the carbide fuel potential.

CARBIDE FUEL PRODUCTION

The carbothermic reduction of the oxides UO_2/PuO_2 was chosen as preparation method, since this process has been proven to be the most economic. In close cooperation with industry a process was developed which, in important steps and equipment, is based on the mixed-oxide pellet fabrication and which only differs, if specific carbide properties make it necessary (inert-atmosphere handling, additional steps for powder and UC-preparation).

In Fig. 2 a comparison of oxide- and carbide-fabrication flow-sheets is given. Keypoint of the carbide preparation, according to the modified procedure developed ("reaction sintering"), is the mixing of pure UC with an intermediate reduction product coming out from the nonquantitative reduction of PuO_2 with carbon (Pu-O-C). The advantages are, that this primary reduction can be performed at a lower temperature, and therefore the losses of Pu are less, and that the UC can be produced by a separate process without Pu-hazard penalties.

Most of the research work was concentrated to improve the fuel quality with respect to a reduction of impurity content (N,O) and of the carbon-rich phases (M_2C_3, MC_2). For this reason thermogravimetric studies of reaction kinetics were performed, and variations of process parameters were reduced by automatic control of production steps (i.e. CO/CO_2-formation during carbothermic-reduction).

The planning of full-size carbide fuel assembly irradiations made it necessary to scale up the existing fabrication capacity. This was done together with industry during 1975/76, and at present a pilot-plant with a capacity of 400 kg (U,Pu)C/year is tested with UC and will come into full operation with the mixed carbide in 1977. Future research work will be shifted from scientific to more technological problems. These are mainly connected with an always safe operation of the carbide-line taking into account the higher throughput of material, and especially the easy combustibility of the carbide material in connection with air-penetration in case of leakage or under abnormal glove box conditions. Furthermore it is important to find a solution for the direct recovery of rejected material without chemical treatment (process economy).

IRRADIATION TESTING OF FUEL PINS

The irradiation experiments performed for the carbide fuel development program (see Fig. 1) were planned to investigate the short-time behavior of fuel pins, the fuel swelling, fission gas release, fuel/cladding compatibility, bonding and high burnup behavior of different types of fuel. The main parameters varied were the fuel pellet density (83 - 96% TD) the type of bonding (He, Ar, Na), the fuel pin diameter (5.6 - 9.5 mm), linear rod power (800 - 1300 W/cm), and burnup (up to 100 MWd/kg M). The cladding material was stainless steel 1.4988 in most cases (0.08% C, 17% Cr, 13% Ni, 1.3% Mo, 1.0% Nb, 0.7% V, 0.1% N), but also 1.4970 (0.1% C, 15% Cr, 15% Ni, 1.2% Mo, 0.45% Ti) and AISI 316 for some fuel pins in DFR mini-subassemblies.

The pins with He-bonding and small gaps between fuel and cladding could not reach high burnup without large cladding strain or even defects (e.g. [1]). This is shown in Fig. 3, where the maximum cladding strains are plotted against burnup. The cladding strains decreased for larger gap width and lower smear density. Pins with very large gaps are still under irradiation or waiting for post-irradiation examination, so that no results are available up to now.

For pins with Na-bonding the cladding strains were small, yet considerable (Fig. 3). Heavy Pu-redistribution towards the outer rim of the pellets was found in three of these pins together with very large interconnected fission gas bubbles and the indication of a central void. These effects are attributed to overheating of the fuel in consequence of gas blanketing in the Na-bonding during irradiation.

Indications of overheating with asymmetrical heat transfer were also observed in pins with Na-bonding in a DFR mini-subassembly. Moreover, a cladding crack occurred, apparently connected with extreme carburization of the cladding.

The evaluation and discussion of the post-irradiation examination results from the irradiated fuel pins is presented in the following paragraphs.

THE CHEMICAL STATE OF IRRADIATED FUEL PINS

Qualitative information on the chemical state of irradiated carbide fuels is given by the microstructure and the α and β-γ autoradiographs of the pin cross sections, resp. (Fig. 4). The α autoradiograph gives indications for actinide redistributions, the β-γ autoradiograph points to local enrichments of β-γ active fission products in the outer fuel region. Concentric rings in the fuel as well as wedges at the fuel surface are visible in both autoradiographs and can be referred to fuel-fission product phases [2].

Transport phenomena

Radial redistribution of uranium and plutonium has been determined quantitatively by microprobe analysis [2,3,4]. No severe plutonium enrichment has been observed in He-bonded mixed carbide fuel. An initial plutonium content of Pu/(U+Pu) = 0.15 resulted in a peak concentration of 0.18 in the region half way to the surface. No burnup dependence of this effect could be ascertained. Peritectic reactions of the fuel with fission products or pin components (thermocouples, absorber discs, etc.) favour plutonium transport to the fuel surface by reason of the rather high plutonium partial pressure of the peritectic melt [4].

Carbon transport by carbon monoxide to the fuel surface and the cladding was observed, the amount of which depends on the oxygen contamination and the stoichiometry of the fuel. Dark oxide precipitates have been identified in pores near the surface of hyperstoichiometric carbide fuels (Fig. 5). The measured Pu/U ratio in these oxide precipitates was 17:72 (wt.%) and was clearly higher than that of the adjacent carbide fuel matrix which was 12:84 (wt %) after 4% burnup [2]. These values agree well with the U-Pu-C-O phase diagram.

Fission product behavior

Phase diagram studies reveal that zirconium and yttrium are soluble in UC and (U,Pu)C, the solubility of molybdenum and the rare earths is limited, the platinum metals form exclusively complex carbides or intermetallic compounds [5].

However, fission product inclusions in carbide fuels are difficult to detect. They are only visible by direct microscopic observation based on proper metallographic techniques. Accumulations of fission product precipitates, due to the migration from the fuel centre region are observed in annular zones which correspond to liquid-solid transformation isotherms of the alloys. The composition of the precipitates depends on the carbon activity of the fuel. Intermetallic phases of actinides, lanthanides and noble metals will only occur in stoichiometric fuels with the appropriate low carbon activity. In hyperstoichiometric fuels $(U,Pu)_2 \cdot (Tc,Ru,Rh)C_{\sim 2}$ precipitates with a higher Pu/U ratio than the adjacent fuel will occur in annular zones (Fig. 6 and 4). $(U,Pu)MoC_{\sim 2}$ precipitates are formed independent of stoichiometry. The alkaline, alkaline earth, and rare earth metals, and technetium form various multicomponent carbides (Fig. 7); the carbon/metal ratios are not known so far. The phases observed to-date are summarized in Table II [2,3]. They agree well with those found by simulation experiments [6,7].

In stoichiometric fuel, the C/M ratio (M ≙ U,Pu) shifts to the MC/M_2C_3 phase boundary during burnup because more carbon is released by the fission process than will be bonded to the fission products. On the other hand, in hyperstoichiometric fuel, the C/M ratio seems to decrease because the rare earth metals form exclusively carbides in this case [7].

ASPECTS FOR CHEMICAL AND MECHANICAL INTERACTION BETWEEN FUEL AND CLADDING

Carburization of the cladding

Carburization of the cladding is the only considerable chemical interaction with the fuel found in carbide fuel pins. Fig. 8 shows carbon concentration profiles, which were measured across the cladding thickness of irradiated pins with Na-bonding and different cladding materials. The measuring method is described in [8].

Fig. 9 shows a more general presentation of the carburization penetration dependent on the cladding temperature, refering to rather disadvantageous conditions with Na-bonding and high carbon content of the fuel. The diagram presents an average of several irradiation and laboratory annealing experiments. With He instead of Na-bonding less carburization occured, often affecting only sectors of the cladding inside circumference.

In subsequent tensile tests on samples from the annealing experiments [9], a stronger strengthening and embrittlement was found as a result of carburization at 600°C than at 700°C, probably because of carbide precipitation coarsening at higher temperatures. Embrittlement was considerably increased by Na-bonding, compared to He-bonding, particularly for high equivalent carbon content of the fuel. The unstabilized high-temperature steel of type 316 was found to be most susceptible to carburization embrittlement.

Swelling, densification, and creep of the fuel

It turned out, that a free swelling rate of about 3 vol % per % burnup has to be allowed for in (U,Pu)C pins of high rod power (about 1000 W/cm). On contact with the cladding, the fuel swelling rate was reduced by cladding restraint, apparently to a range of 1.5 - 1.7 vol % per % burnup. Obviously, there is still a considerable contribution of fission gas bubbles, and even up to 10% burnup one cannot expect saturation of the fission gas swelling by complete release of the fission gas produced. At 10% burnup, the concentration of retained fission gas amounted to about 2×10^{-2} gas atoms per (U+Pu)-atom, while a saturation level of about 1.5×10^{-2} was found in oxide fuel of low temperature (<1100°C).

For fuel pins with He-bonding, cladding plastic strain by fuel swelling has to be expected in general by reason of fuel/cladding contact. Cladding strain can be reduced by irradiation-induced densification and creep of the fuel. At present one can estimate, that for low fuel pellet density of 80 - 85% TD irradiation densification could lead to a final density of about 90% TD. However, the densification rate, related to the fuel burnup, seems to be lower at least by a factor of 10 than for oxide fuel of equal porosity. Consequently, irradiation-induced creep appears to be more important. Since the irradiation creep rate of carbide fuel seems to be lower by a factor of about 10 than for oxide fuel under comparable conditions, cladding strain in carbide fuel pins will sensitively depend on the fuel/cladding creep strength ratio.

In this connection, the fuel porosity seems to be an important parameter. Fig. 10 shows the correlation of the cladding strain measured, the fuel creep rate estimated, and the fuel pellet density for results from thermal reactor tests like those in Fig. 3. Fuel of very low smear density <80% TD should be required to guarantee sufficiently small cladding strain up to high burnup. Apparently, a considerable fraction of the porosity dependence is due to a fuel strength reduction (unlike fuel densification). Consequently, stronger cladding tubes should make it possible to achieve higher burnups.

DESIGN OF A CARBIDE FUEL ASSEMBLY

In order to conduct integral performance tests, two identical carbide fuel assemblies will be prepared for the second core of the Karlsruhe fast test reactor KNK II. Their layout largely corresponds to the KNK II oxide assemblies; the same type of structural components is used. The hexagonal wrapper tube has an internal width across flats of 118.9 mm and a corner radius of about 23 mm. This tube accommodates 121 fuel rods of 8.5 mm diameter with a pitch of 10.35 mm. The six corner positions are occupied by structural rods. Together with 7 spark-eroded grid spacers, they form the bundle structure. The fuel stack length is 600 mm with a 200 mm blanket on its top and bottom each. The fission gas plenum of about 467 mm length has been provided on the lower, cold end. With a maximum nominal rod power of 800 W/cm a fuel assembly power of about 4.15 MW will be obtained.

A summary of the essential pin design parameters is contained in Table III. The main problems in fuel pin design are related to the heat transfer in the gap. According to [10], the heat transfer coefficient amounts to about 0.4 W/cm^2K for fabrication gap widths of about 400 μm and a rod power of 650 W/cm. This is approximately in line with results from FR 2 tests in Karlsruhe [11]. So, if $\chi_{max,nom}$ is limited to 600 W/cm during startup, which corresponds to $\chi_{max,extr.}$ of about 750 W/cm, the limit of 1800°C in the fuel is not substantially exceeded even under hot channel conditions. Due to the formation of heat bridges caused by fuel pellet rupture, a clear improvement of the heat transfer to about 1 W/cm^2K is obtained within a few days already [10,11].

According to the high pin power, the thermal stresses are considerable in the cladding. Values of about 200 N/mm^2 are achieved. However, this is not critical in case the number of thermal cycles is kept low. Since the free swelling rate of the fuel is rather high, the gap between fuel and cladding will be closed before major amounts of fission gas have been released. Thus, the influence of fission gas on heat transfer can be neglected.

The cladding strain caused by fuel swelling decreases with the fuel smear density (see above). A cladding diameter increase between 0.5 and 1% has to be expected up to a maximum burnup of 70 MWd/kg M for a smear density of 75% TD. The main contribution to cladding stress is made by the contact pressure of the swelling fuel, which is expected to be about 20 MPa. By contrast, the fission gas pressure can be neglected. At the target burnup 2 MPa have to be expected for 40% fission gas release.

REFERENCES

[1] FREUND, D., ELBEL, H., STEINER, H., GfK Rep. KFK 2268 (1976)

[2] KLEYKAMP, H., Reaktortagung, Düsseldorf, 30 March - 2 April 1976, ZAED, Leopoldshafen (1976) 542

[3] KLEYKAMP, H., J.Nucl.Mater. 47 (1973) 271

[4] WEIMAR, P., KLEYKAMP, H., POLITIS, C., Atomwirtschaft 19 (1974) 235

[5] HOLLECK, H., Thermodynamics of Nuclear Materials 2, IAEA, Vienna (1974) 213

[6] HOLLECK, H., SMAILOS, E., THUEMMLER, F. Reaktortagung, Berlin, 2 - 5 April 1974, ZAED, Leopoldshafen (1974) 384

[7] SMAILOS, E., GfK Rep. KFK 1953 and EUR FNR-1179 (1974)

[8] PIERCE, T.B. et al., Nuclear Instruments and Methods 118 (1974) 115

[9] GOETZMANN, O., HOFMANN, P., SARIKAYA, Y., GfK Rep. KFK 1942 (1973) and KFK 1993 (1974)

[10] MIKAILOFF, H., Bulletin d'Informations Scientifiques et Techniques 196 (1974) 49

[11] WEIMAR, P., FIEDLER, H., GfK Rep. KFK 1919 (1974).

TABLE I: Reference data for SNR carbide fuel element

Fuel Material : (U,Pu)C-pellet Smear density : 75% TD Bonding : helium	**Blanket** Material : UC-pellet Density : 95% TD
Cladding Material : 1.4970; c.w., a. Diameter : 8.0 mm Wall-thickness : 0.55 mm	**Operational conditions** Linear rating : 800 W/cm Specific power : 300 W/g Midwall clad-temp.: 650°C max. Discharge burnup : 70 MWd/kgM

TABLE II: Observed fission product phases in stoichiometric and hyperstoichiometric carbide fuel (M = U,Pu)

	MC	MC_{1+x} $(MC+M_2C_3)$
Fuel matrix	(M,Y,Zr,Mo,La,...,Sm)C	$(M,Y,Zr,Mo,La,...,Sm)C_{1+x}$
Inclusions	$(M,La,...,Sm)_3 \cdot (Tc,Ru,Rh)_4$ $(M,La,...,Sm) \cdot (Tc,Ru,Rh)$ $MMoC_{\sim 2}$ (La,...,Nd)-carbide (Sr,Ba,Ce)-carbide	$M_2(Tc,Ru,Rh)C_{\sim 2}$ $MMoC_{\sim 2}$ (La,...,Sm)-carbide (Cs,Sr,Ba,Ce)-carbide (M,Sr,Y,Zr,Ba,Ce)-carbide (Cs,Ba,Tc,La,Ce)-carbide $(Sr,Ba)Pd_x$

Table III: Pin design parameters for KNK subassemblies

Pu-percentage	15 wt %
U-235-enrichment	69 % U
Pellet density	84 % TD
Pellet diameter	7.00 mm
Rod Power $\chi_{max.nom.}$	800 W/cm
$\chi_{max.extr.}$	990 W/cm
Target burnup	70 MWd/kg M
Neutron dose (E >0.1 MeV)	$4.7x10^{22} n/cm^2$
Cladding dimensions	8.5x0.55 mm
Cladding material	1.4970 ss, 15% cw, 800°C/2h
Cladding midwall temp. max.extr.	685°C

Experiment Type	Objectives	Reactor	1970	1975	1980
Single Pin Irradiations	Basic Parameter Tests for - Mater. Data Evaluation - Fuel/Pin Behaviour - Concept Comparison	FR-2 (Thermal) BR-2 (Epitherm.)	30 pins 20 pins		
Small Bundle Tests	Fuel/Pin Behaviour under Fast Flux Conditions Testing of Reference Concept	DFR (Mini-Sub-assembly) PFR (DMSA)	3x7 pins	2x7 pins	
Safety Tests	Non Steady State Tests with Overpower, Power-cycling, Loss-of-coolant	HFR		8 pins	
Original Fuel Element	Bundle Behaviour	KNK-II SNR-300		2x121 p.	2x169 p.

Fig. 1: Status and planning of carbide irradiation experiments

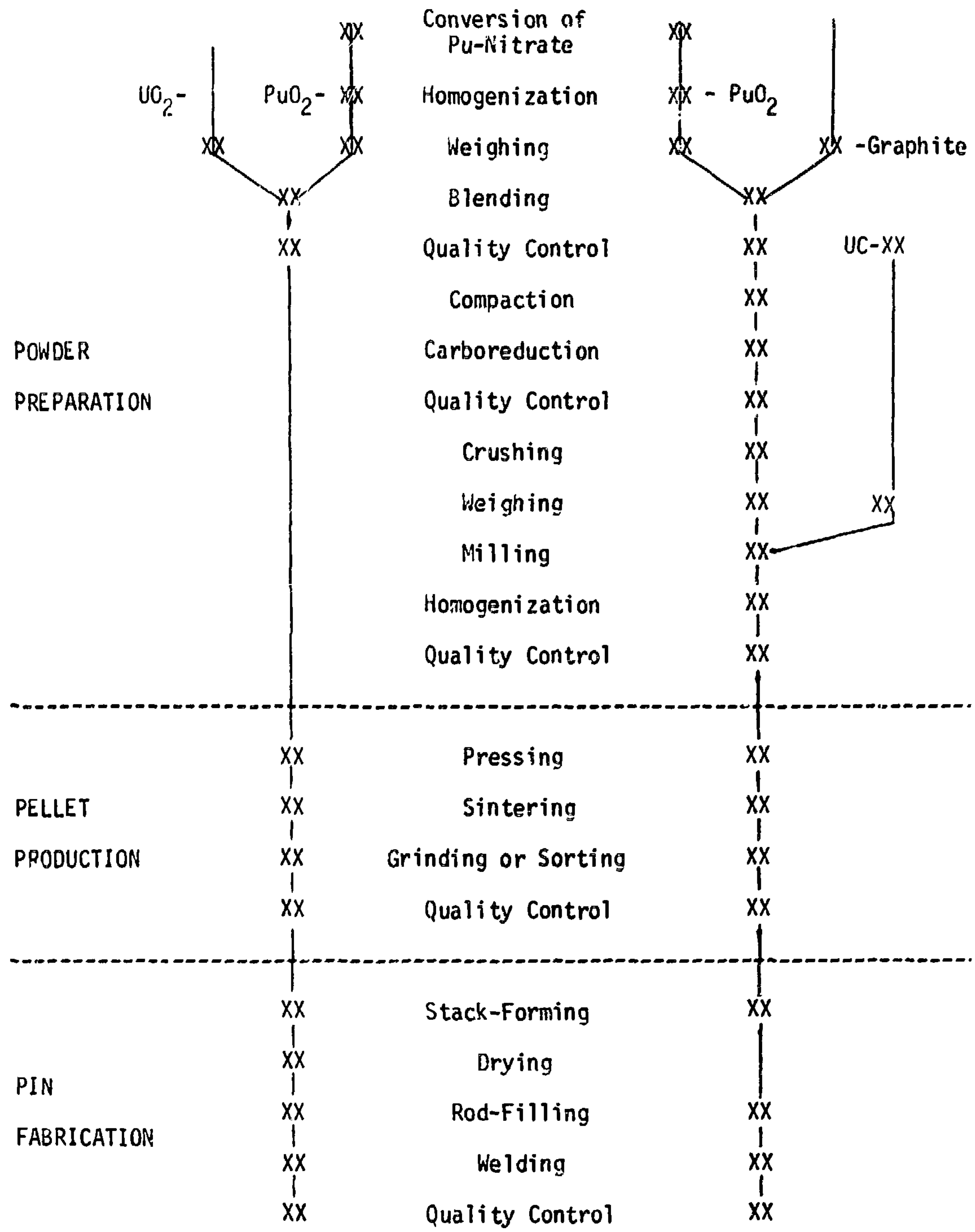

Fig. 2: Fabrication flow sheets for mixed (U,Pu) oxide and mixed (U,Pu) carbide

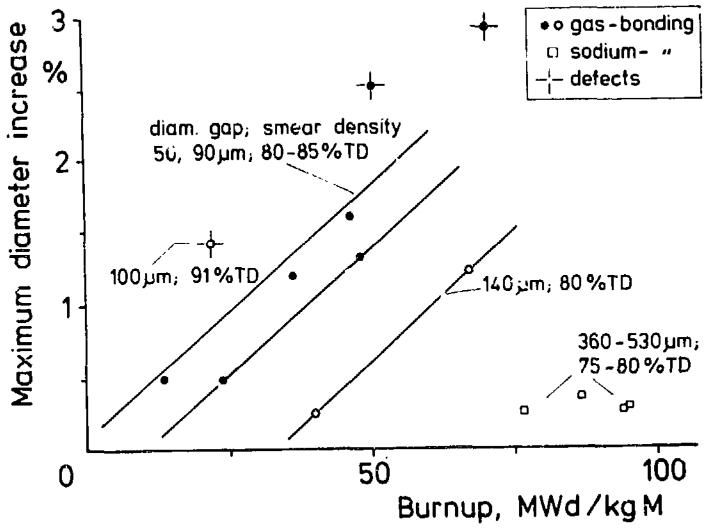

Fig. 3: Maximum cladding diameter increase of carbide fuel pins of different fuel density and bonding, after irradiation in thermal test reactors

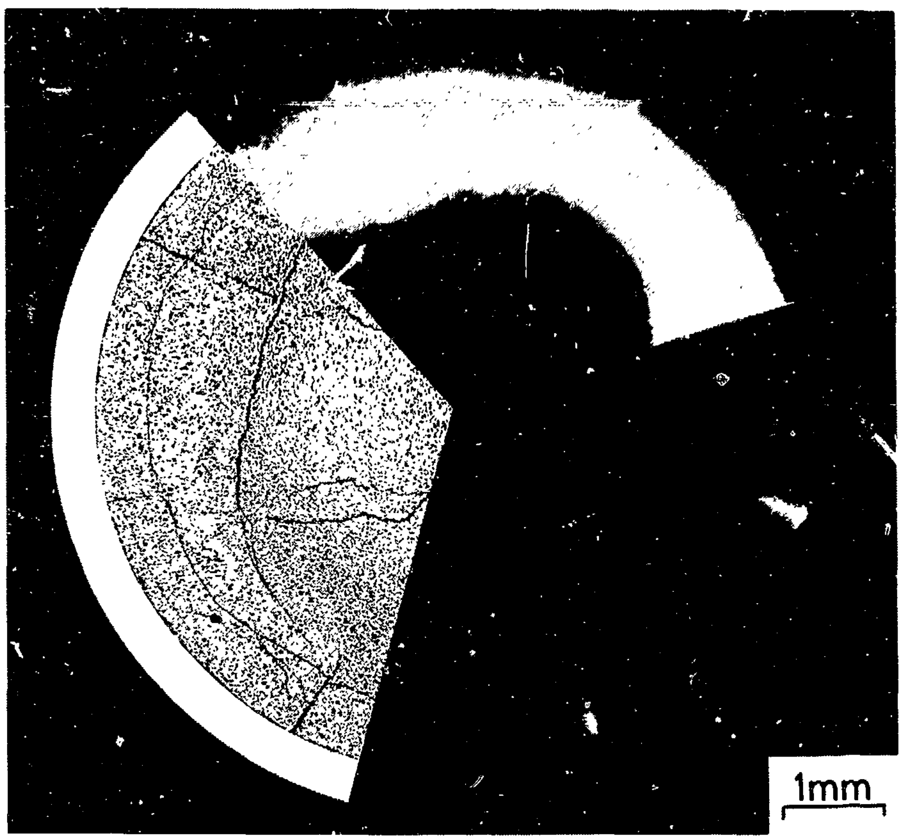

Fig. 4: Microstructure, α autoradiograph, and ß-γ autoradiograph of a mixed carbide fuel pin cross section; epithermal neutron irradiation, linear power 1070 W/cm, burnup 4.0%

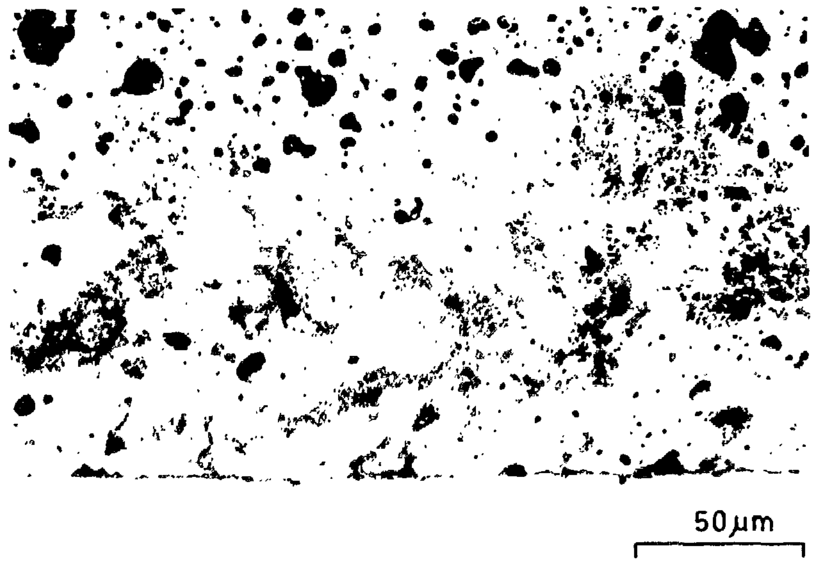

Fig. 5: Mixed oxide precipitates (dark phases) near the surface of mixed carbide fuel

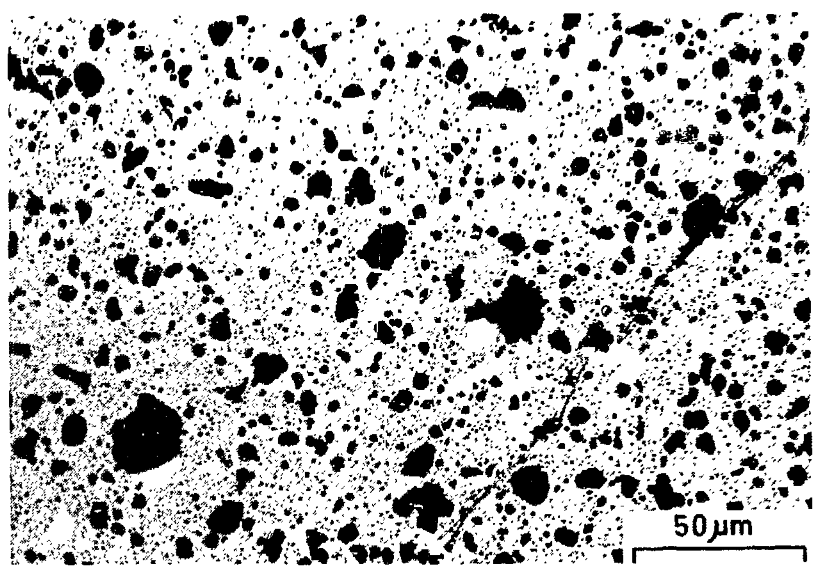

Fig. 6: $(U,Pu)_2 \cdot (Tc,Ru,Rh)C_{\sim 2}$ inclusions (bright phases) in hyperstoichiometric mixed carbide, burnup 7%

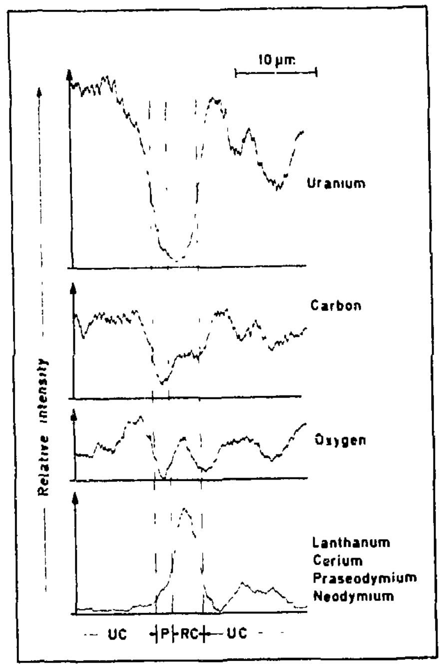

Fig. 7: Relative concentration profiles of a rare earth carbide inclusion (RC) in irradiated UC, burnup 4%; P = pore

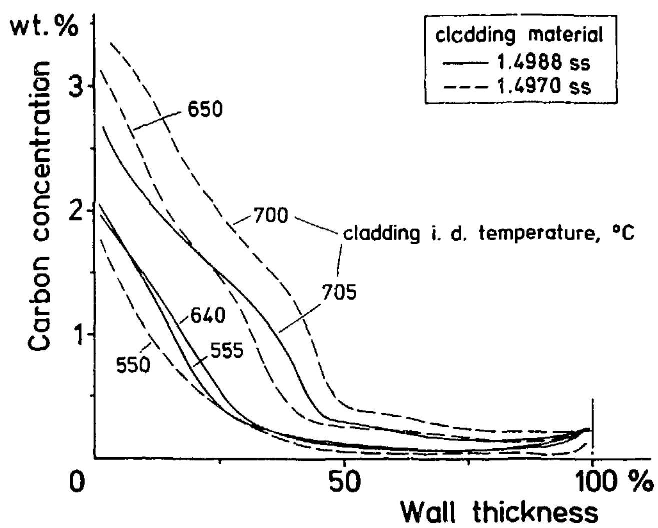

Fig. 8: Cladding carburization profiles in Na-bonded (U,Pu)C pins measured after DFR irradiation to about 5% burnup

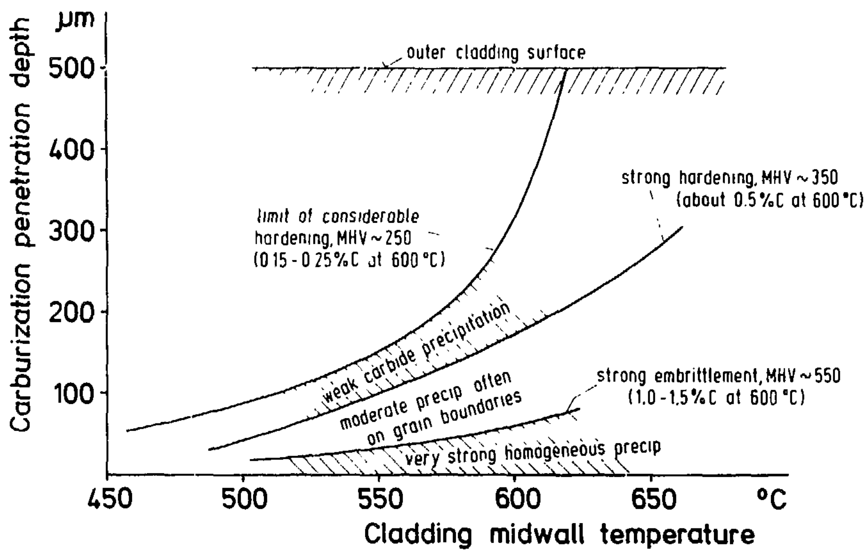

Fig. 9: Carburization of stainless steel cladding by high-carbon fuel (equivalent carbon content >5.15%) with Na-bonding in about 5000 h

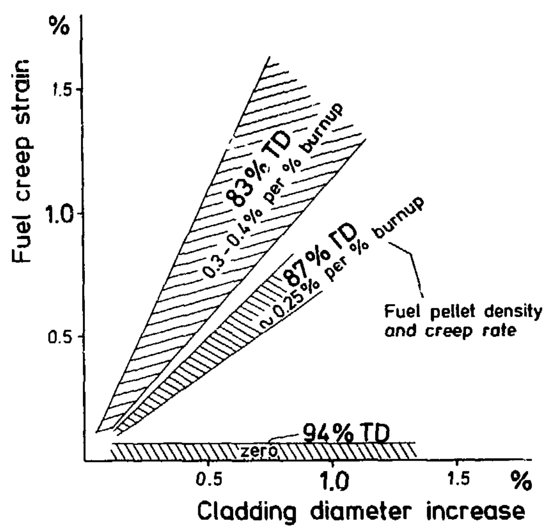

Fig. 10: Correlation of cladding strain and (U,Pu)C irradiation creep dependent on fuel density, under thermal test reactor irradiation